

# SOFT X-RAY ABSORPTION SPECTROSCOPY OF THE MgB<sub>2</sub> BORON K EDGE IN AN MgB<sub>2</sub>/Mg COMPOSITE

D. A. FISCHER

Materials Science and Engineering Laboratory,  
National Institute of Standards and Technology,  
Gaithersburg, Maryland 20899, USA  
daniel.fischer@nist.gov

A. R. MOODENBAUGH\*, QIANG LI, G. D. GU, YIMEI  
ZHU, J. W. DAVENPORT and D. O. WELCH

Brookhaven National Laboratory, Upton, NY 11973-5000, USA  
\*moodenba@bnl.gov

HAIBIN SU

Division of Materials Science, Nanyang Technological University,  
50 Nanyang Avenue, Singapore 639798  
HBSu@ntu.edu.sg

Soft X-ray absorption spectroscopy (XAS), using fluorescence yield, was used to study the boron K near edge in MgB<sub>2</sub> superconductor. The sample consists of MgB<sub>2</sub> crystallites randomly oriented in a magnesium matrix. Abrasion of the sample surface in vacuum provides a surface relatively free of boron-containing impurities. The intrinsic boron K near edge spectrum of the sample at a temperature of 295 K is identified. This spectrum is then compared in detail with a spectrum calculated using the full potential linearized augmented plane wave method. Features predicted by the theory appear near the expected energies, with qualitative agreement regarding shape and intensity.

*Keywords: Soft X-ray absorption; MgB<sub>2</sub>; superconductor.*

## 1. Introduction

MgB<sub>2</sub>, a superconductor with transition temperature  $T_c = 39$  K, has attracted much attention recently.<sup>1</sup> In many respects this material can be viewed as a model intermetallic compound with high  $T_c$ . The chemical structure is relatively simple. Calculations of electronic structure can be expected to be reliable and informative, and spectroscopic studies of the boron K edge should provide a basis for evaluating the quality of those calculations. More recently, several potential superconducting applications have been proposed.

The boron K X-ray absorption spectroscopy (XAS) of polycrystalline MgB<sub>2</sub> has been the subject of several studies.<sup>2-5</sup> The energies needed, in the range  $180 \text{ eV} < E < 220 \text{ eV}$ , are relatively low. Even X-ray fluorescence experiments, often considered to be bulk-sensitive, are restricted to within about 500 nm of the surface. The XAS spectra feature a prominent prepeak near  $E = 186.4 \text{ eV}$ . The main edge jump appears near  $E = 191 \text{ eV}$ . For polycrystalline samples, in the range  $191 < E < 195 \text{ eV}$ , several features appear which vary from sample to sample. Oriented film measurements have provided more complete information, including angle dependence of the XAS spectrum.<sup>6</sup> Results from at least one single crystal measurement<sup>7</sup> are more comparable to those obtained from typical polycrystalline samples. A portion of the data reported in this work was published in conjunction with an electron energy loss spectroscopy study which provided direction-dependent data from individual crystallites.<sup>8</sup> In that work the major features of the B near edge are similar to those reported in the oriented film work.<sup>6</sup>

The inconsistency of published results of polycrystalline samples, and of some measurements on crystals, strongly suggests that MgB<sub>2</sub> materials commonly contain either bulk or surface boron-containing impurities. These impurities may have implications on the stability of practical conductors in potential applications. This study began with preparation of a dense composite sample consisting of MgB<sub>2</sub> crystallites ( $T_c = 39$  K) in a magnesium metal matrix. Prior to exposure in the vacuum, the dense matrix protects the unexposed interior bulk MgB<sub>2</sub>. We prepared a fresh surface by abrasion using a specially designed tool mounted in the vacuum chamber. We obtained fluorescence yield (FY) data on this composite MgB<sub>2</sub> sample. This XAS data is supplemented by surface sensitive partial electron yield data on the dense MgB<sub>2</sub> sample, and by FY measurements on commercial powder MgB<sub>2</sub>, BN, and boron oxide.

These XAS measurements can be viewed as experiments which fulfill two distinct goals. XAS is useful both as a fundamental probe of electronic structure and as a powerful materials characterization tool. The experiments on clean samples probe the electronic structure and provide a desirable high resolution experimental validation of MgB<sub>2</sub> band structure calculations. The experimental results here are consistent with EELS, and film measurements.<sup>6</sup>

The XAS measurements near the boron K edge (180220 eV) are sensitive to impurities that standard techniques might not detect. For example, X-ray diffraction of MgB<sub>2</sub> powder typically shows a reasonably pure MgB<sub>2</sub> pattern. Because boron oxides or nitrides may be nearly amorphous, and are composed of light elements, a significant impurity component would likely be difficult to identify

using X-ray diffraction. Neutron diffraction might normally be a useful, easily accessible characterization method. However, in the case of boron-containing compounds, isotopically pure boron is required for specimens planned for neutron studies. These XAS studies provide information on light element impurities that are difficult to obtain through other means.

The band structure calculations are performed using the full potential linearized augmented plane wave (FLAPW) method, as implemented in the WIEN97 code.<sup>9</sup> The procedures are similar to previously published work.<sup>2,10,11</sup> First we evaluate the boron K edge XAS experiments thoroughly. Based on this ground work, the features of the MgB<sub>2</sub> near edge are compared with the experimental calculations.

## **2. Experimental Procedure**

The dense composite MgB<sub>2</sub>/Mg sample used for the primary XAS measurements was prepared using a significant excess of Mg.<sup>12</sup> The sample has a  $T_c = 39$  K. For the initial experiments, the sample surface was abraded in air before introduction into the vacuum chamber. Preliminary boron K XAS data suggested that this sample surface was not optimally clean using this procedure. Consequently, a tool was fabricated and installed into the experimental chamber to allow abrasion of the sample surface (cleaning *in situ*) in the ambient vacuum, pressure  $p \approx 10^{-5}$  Pa, without necessitating a subsequent exposure to air.

The boron XAS measurements were performed at the NIST/Dow Materials Characterization Facility at the Brookhaven

National Laboratory National Synchrotron Light Source (NSLS) beamline U7A. The energy resolution of the incident photons is 0.2 eV. The position of the carbon K edge was used to establish the energy calibration. There was no perceptible shift in energy scale in these experiments ( $\Delta E < 0.1$  eV) as long as the monochromator setup was not changed. The fluorescence yield data was obtained using a gas-proportional counter.<sup>13</sup> Partial electron yield data were obtained simultaneously in some cases.

It is most desirable to determine a background signal in the pre-edge region to establish a baseline to be subtracted from the data. Usually fluorescence yield data are quite stable and the baseline is reliably defined. Several factors prevented an accurate determination of background for subtraction at the boron K edge in these studies. First, beamline hardware limitations prevented the study of photon energies below 184 eV. Second, there is an unexpected positive slope to the fluorescence signal in the 2 eV interval above the low energy limit, 183.8 eV, but below the first prepeak. This may be due to a signal from the third harmonic of oxygen ( $E \approx 550/3$  eV). The incident photon flux  $I_0$  was monitored by the total electron yield from a clean gold grid positioned in the incident photon beam. Over the energy range of interest,  $183.8 \text{ eV} < E < 220 \text{ eV}$ ,  $I_0$  changes by about an order of magnitude. While a normalization is made to account for the varying  $I_0$  as part of the data analysis, the correction may not be as reliable here as it is in cases where  $I_0$  varies less drastically. Consequently, in this work we present data without having performed background subtractions.

### 3. Theoretical Calculations

The MgB<sub>2</sub> partial density of states and XAS spectrum were obtained using the full potential linearized augmented plane wave method, calculated by the WIEN97 computer code.<sup>9</sup> For the calculation procedure, initial adjustments involved varying the total energy, based on changes in hexagonal parameters, c<sub>0</sub>/a<sub>0</sub> ratio and cell volume. Minimum energy was achieved for a<sub>0</sub> = 0.3081 nm and c<sub>0</sub> = 0.3528 nm.

This agrees well with the experimental data, a<sub>0</sub> = 0.3086 nm and c<sub>0</sub> = 0.3521 nm.<sup>11</sup> The total density of states (DOS)

$$D(E) = \frac{1}{N} \sum_i \delta(E - \varepsilon_i) \quad (1)$$

measures the number of eigenstates  $\varepsilon_i$  between E and dE throughout the crystal. Furthermore, it is useful to project the total density of states onto a local set of states and examine the overlap of each eigenstate  $|i\rangle$  with the local state  $|a\rangle$ . The probability of finding an electron in the eigenstate  $|i\rangle$  at site  $|a\rangle$  is  $|\langle a|i\rangle|^2$ . Thus the local contribution to the density of states from site  $|a\rangle$  is<sup>14</sup>

$$D_a(E) = \sum_i |\langle a|i\rangle|^2 \delta(E - \varepsilon_i). \quad (2)$$

This expression can be decomposed by angular momentum inside the muffin tin spheres such that the density of s-, p-, d-, ... states may be calculated. Local rotation matrices are used for the implementation of site symmetry for each atomic site. This can provide a clear physical interpretation of the decomposition of charge density with angular

momentum for a proper orientation of the coordinate system.<sup>9</sup> In MgB<sub>2</sub> the point group of boron is C<sub>3v</sub>. Thus the 2p orbitals split into two irreducible representations A<sub>1</sub> and E. The corresponding bases are those calculated in this work, 2p<sub>z</sub> and (2p<sub>x</sub>, 2p<sub>y</sub>) respectively. The differential photoionization crosssection<sup>15</sup> is given by

$$\frac{d\sigma}{dE} \propto \sum_f |\langle \Phi_f | \mathbf{P} \cdot \mathbf{A} | \Phi_i \rangle|^2 \cdot \delta(E_f - E_i - \hbar\omega), \quad (3)$$

where  $\mathbf{A}$  is the polarization of the incident photon and  $\mathbf{P}$  is the momentum operator.

Since the core hole corresponding to the boron K edge is well localized inside the muffin tin sphere, the important boundary conditions are the atomic ones, such as the requirement that the radial wave function vanishes at the nucleus and orthogonality to the core level. It is possible to calculate the above matrix element only inside the muffin tin portion. This provides a basis for comparing the projected density of states with an experimental spectrum. Finally, the calculated XAS spectrum was broadened to account for the XAS experimental energy resolution and lifetime broadening, using an 0.2 eV full width at half-maximum Gaussian function.

#### 4. Results

The primary result of this study is the fluorescence yield (FY) XAS signal of the boron K edge of clean MgB<sub>2</sub>. In most cases, several energy scans are summed in order to improve statistics. An individual energy scan took about 1 hr. Figure 1 shows three summed spectra, stacked, for the composite MgB<sub>2</sub>/Mg sample. The

uppermost plot 1(c) is taken in the case where surface had been abraded before the sample was introduced into the vacuum. The peak near 186.4 eV and the edge jump near 191 eV are intrinsic MgB<sub>2</sub> features, generally observed and in good agreement with calculations.<sup>2-5</sup> An additional significant peak is observed at 193.6 eV, with a smaller peak at E = 191.5 eV, similar to some previously published results. The data of Fig.1(a) is taken relatively soon (within two hours) after cleaning was performed *in situ*. The peak at 193.6 is reduced noticeably, and the feature at 191.5 eV has been essentially eliminated. Figure 1(b) shows the XAS signal of the same sample, but at least two hours after cleaning *in situ*. The results are comparable to those of Fig. 1(a), with the exception of the peak at 193.6 eV. The intensity of this peak has grown with time.

We now look more closely at the FY behavior of the sample abraded *in situ*. Following one MgB<sub>2</sub> surface cleaning, a series of energy scans were performed over a period of about 9.5 hours. In Fig. 2 we plot the net integrated intensities of the MgB<sub>2</sub> prepeak near 186.4 eV and the peak at 193.6 eV as a function of time after surface cleaning. We find the MgB<sub>2</sub> prepeak to decrease in intensity with time and the peak at 193.6 eV to increase. This indicates that the peak at 193.6 is due to a surface impurity developing in the 10<sup>-5</sup> Pa vacuum environment. We also note that the intensity of this peak does not extrapolate to zero intensity at the time of cleaning (time = 0 h), but has significant predicted intensity at the initial time. This suggests that the cleaning process may not be fully optimized, or that there may be a minor impurity component inherent in the bulk of the as-prepared sample. It is also conceivable that a small intrinsic

feature occurs at the same intensity as this impurity peak, or that the rate of change of intensity of the peak increases more rapidly immediately after cleaning. This is unlikely though, since neither theory nor results of Ref. 6 show a similar feature. There is an apparent reduction in intensity with time of the  $\text{MgB}_2$  prepeak at 186.4 eV (also in Fig. 2). The surface may be developing a coating which reduces the observed intensity of the  $\text{MgB}_2$  signal. This is indirect evidence that the impurity phase is surface-related. Near the energy of the second impurity peak,  $\sim 191.5$  eV, the spectrum is stable after cleaning. We conclude that the remaining intensity near this energy is attributable to the  $\text{MgB}_2$  spectrum.

Figure 3 contains FY results for an alternate sample of  $\text{MgB}_2$ , a pressed pellet of commercial powder. The XAS for this sample bears similarities to those reported by McGuinness et al.<sup>2</sup> Also displayed are results for BN and for a boron oxide sample. The BN displays a major peak at 191.5 eV and another at 193.6 eV, similar in position but with different intensity ratio compared to those observed in the powder. The boron oxide shows a feature at 193.6 eV, similar to that observed in the dense sample (Fig. 1). It appears that the peak at 191.5 eV in  $\text{MgB}_2$  powder may be attributable to BN while that at 193.6 may be due primarily to boron oxides.

The partial electron yield (EY) results are very surface sensitive, and thus helpful in evaluating the degree of surface impurity. Additionally the EY results can be compared to other published results. Figure 4 contains EY results for our dense sample. The data taken after *in situ* cleaning show a definite  $\text{MgB}_2$  prepeak, a feature absent in the sample cleaned in air. This prepeak is reduced in

intensity from that observed in FY. In previously published work, either a small prepeak<sup>3</sup> or no prepeak was seen in EY.<sup>4</sup> The peak at 193.6 eV attributed to boron oxides appears in both spectra, but is noticeably suppressed for the sample cleaned *in situ*.

## 5. Comparison with Theory

The XAS spectrum (Fig. 5(b)), calculated using FLAPW formalism implemented in the WIEN97 code, includes an instrumental broadening of  $\sim 0.2$  eV, approximating the energy resolution of the XAS experiment. The separate  $p_z$  and  $p_{x+y}$  contributions to the partial density of states are shown in the upper panel (5(a)). In order to easily compare features of the calculated spectrum to the experimental XAS in Fig. 5(b), the calculated prepeak energy, intensity, and a flat background were adjusted to coincide with the experimental peak near 186.4 eV. The calculated prepeak is similar in shape to the experimental peak. Next, the relatively flat region 187–190 eV is reasonably accurately described, attributable to a  $p_z$  contribution. The main edge position and amplitude near 191 eV are fairly well accounted for.

Calculated peaks near 192.5 and 194.5 eV (primarily  $p_{x+y}$  contribution) are represented in the data, but less prominent than predicted by theory. Note that the adjacent experimental peak, near 193.6 eV, is most likely due to oxide impurity. A general characteristic in the post-edge region is that calculated features are more prominent and well defined than those actually observed in the experimental spectrum. Above 195 eV the agreement between experiment and calculation can only be characterized as fair. A decrease in intensity

observed near 204 eV appears to be predicted by theory.

## **6. Summary**

The characteristic features of the boron K near edge are delineated in this XAS fluorescence yield study of  $\text{MgB}_2$ . The literature gives a broad range of  $\text{MgB}_2$  boron K edge XAS results for polycrystalline samples. The present FY results for a dense sample with surface cleaned in the vacuum chamber provide reliable results for randomly oriented material. The comparison of the experimental data with theory shows several areas of reasonable agreement as described in the previous section. However, many above-edge features calculated to be sharp and prominent, are observed as weak or broad experimental XAS features.

The experimental data presented in this work facilitates a more reliable comparison to theory. We feel that the theory is not predictive to the degree that was hoped. This clear comparison for a relatively simple model compound  $\text{MgB}_2$  may provide a path for improving the theoretical approach. Future improvements in the XAS fluorescence experiment should include a better understanding of the energy dependence of the background signal so it might be subtracted from the data.

## **Acknowledgments**

Zugen Fu helped with the NSLS U7A setup. Doug Gillette built the vacuum-compatible abrasion tool. The work at Brookhaven National Laboratory, including use of the National Synchrotron Light Source, is supported by the U.S. Department of Energy, Office of

Science, Office of Basic Energy Sciences, under Contract No. DE-AC02-98CH10886. Certain commercial names are identified in this paper for purposes of clarity in presentation. Such identification does not imply endorsement by the National Institute of Standards and Technology.

## References

1. J. Nagamatsu, N. Nakagawa, Y. Z. Murakana, Y. Zenitani and J. Akimitsu, *Nature* **410** (2001) 63.
2. C. McGuinness, K. E. Smith, S. M. Butorin, J. H. Guo, J. Nordgren, T. Vogt, G. Schneider, J. Reilly, J. J. Tu, P. D. Johnson and D. K. Smith, *Europhys. Lett.* **56** (2001) 112.
3. R. F. Klie, H. B. Su, Y. Zhu, J. W. Davenport, J. Idrobo, N. D. Browning and P. D. Nellist, *Phys. Rev. B* **67** (2003) 144508; E. Z. Kurmaev, L. I. Lyakhovskaya, J. Kortus, A. Moewes, N. Miyata, M. Demeter, M. Neumann, M. Yanagihara, M. Watanabe, T. Muranaka and J. Akimitsu, *Phys. Rev. B* **65** (2002) 134509.
4. T. A. Callcott, L. Lin, G. T. Woods, G. P. Zhang, J. R. Thompson, M. Paranthaman and D. L. Ederer, *Phys. Rev. B* **64** (2001) 132504.
5. J. Nakamura, N. Yamada, K. Kuroki, T. A. Callcott, D. L. Ederer, J. D. Denlinger and R. C. C. Perera, *Phys. Rev. B* **64** (2001) 174504.
6. G. P. Zhang, G. S. Chang, T. A. Callcott, D. L. Ederer, W. N. Kang, E.-M. Choi, H.-J. Kim and S.-I. Lee, *Phys. Rev. B* **67** (2003) 174519.
7. J. Nakamura, S.-Y. Nasubida, E. Kabasawa, H. Yamazaki et al., *Phys. Rev. B* **68** (2003) 064515.
8. Y. Zhu, A. R. Moodenbaugh, G. Schneider, J. W. Davenport, T. Vogt, Q. Li, G. Gu, D. A. Fischer and J. Taftø, *Phys. Rev. Lett.* **88** (2002) 247002.
9. P. Blaha, K. Schwarz and J. Luitz, WIEN97, Vienna University of Technology (1997); P. Blaha, K. Schwarz, P. Sorantin and S. B. Trickey, *Computer Phys. Comm.* **59** (1990) 399.
10. J. M. An and W. E. Pickett, *Phys. Rev. Lett.* **86** (2001)

4366.

11. T. Vogt, G. Schneider, J. A. Hriljac, G. Yang and J. S. Abell, Phys. Rev. B 63 (2001) 020505.
12. Q. Li and G. Gu, unpublished.
13. D. A. Fischer, J. Colbert and J. L. Gland, Rev. Sci. Instrum. 60 (1989) 2596.
14. D. A. Muller, D. J. Singh and J. Silcox, Phys. Rev. B 57 (1998) 8181.
15. J. W. Davenport, Phys. Rev. Lett. 36 (1976) 945.

## List of Figures

Fig. 1. Fluorescence yield for dense composite  $\text{MgB}_2/\text{Mg}$ . (a) Sample measured soon after cleaning in vacuum. (b) Sample cleaned in vacuum  $>2$  hr prior to measurement. (c) Sample cleaned in air before introduction into the vacuum chamber. Data (b) and (c) were shifted up the vertical scale for clarity of presentation.

Fig. 2. Time dependence of  $\text{MgB}_2$  boron K edge features for dense composite. Bottom: Time dependence of 193.6 eV peak, identified as a surface impurity, with time. Top:  $\text{MgB}_2$  186.4 eV prepeak intensity as a function of time. Lines through the data are linear square fits. Inset shows a sample spectrum (time = 9.5 h) illustrating the areas used to calculate the peak intensities.

Fig. 3. FY boron K edge for (a) powder  $\text{MgB}_2$  (b) boron oxide, and (c) boron nitride (BN). Data sets (b) and (c) were shifted up the vertical scale for clarity of presentation.

Fig. 4. Surface sensitive electron yield (EY) for  $\text{MgB}_2$  boron K edge of dense composite (a) after cleaning in vacuum and (b) after cleaning in air. Trace (b) was shifted up the vertical scale for clarity of presentation.

Fig. 5. Comparison of XAS boron K edge for  $\text{MgB}_2$  composite to the calculated spectrum. Top panel (a) shows partial density of states (PDOS) calculations for boron  $p$  orbitals. In the bottom panel (b) the experimental boron K XAS spectrum is compared to a calculated spectrum based on the PDOS calculations.

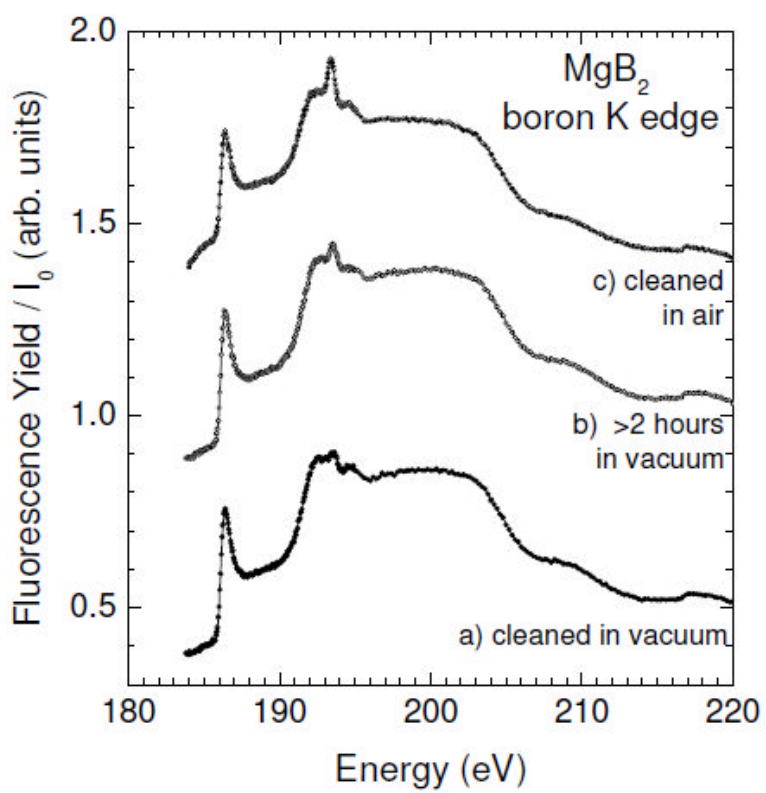


Fig. 1

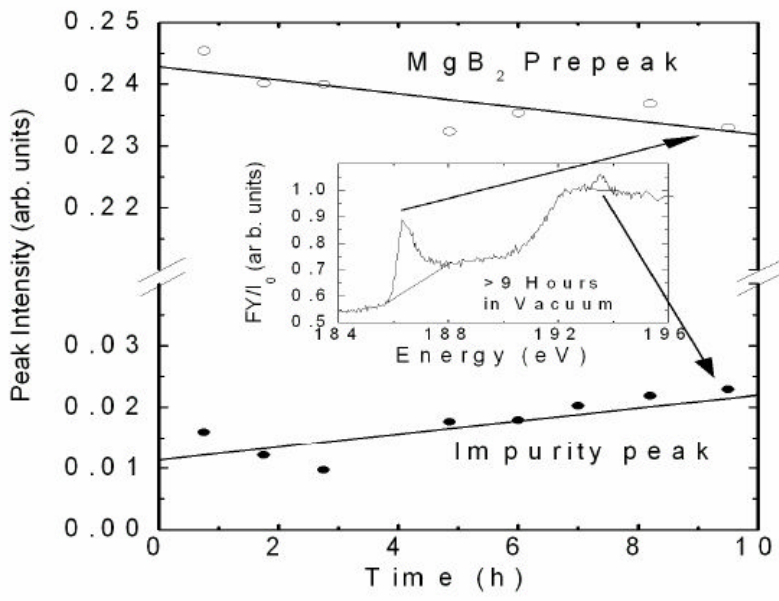


Fig. 2

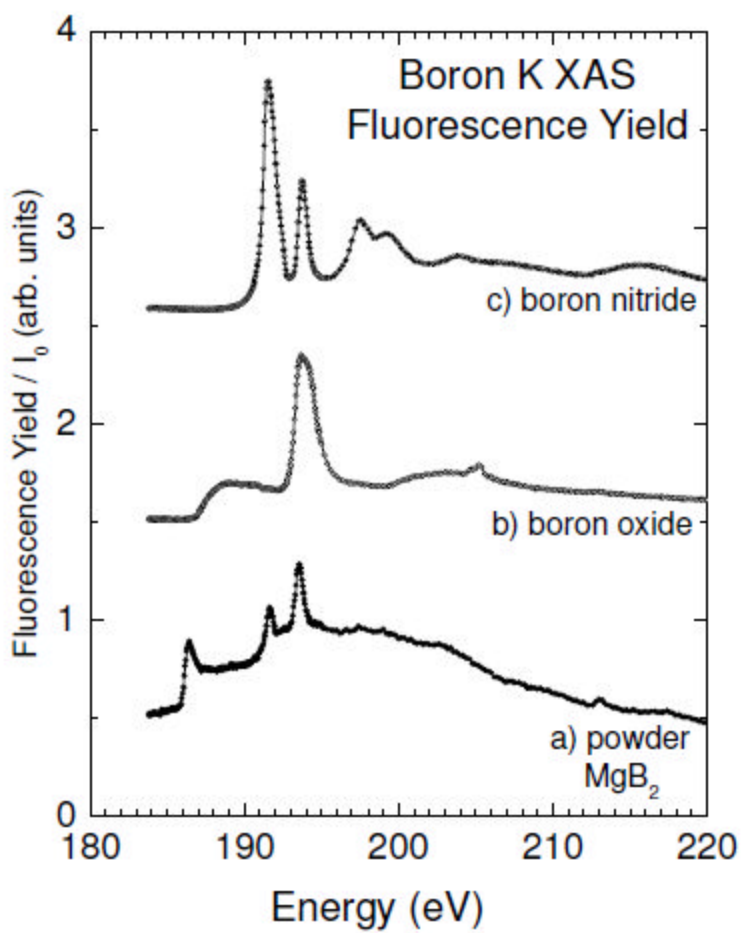


Fig. 3

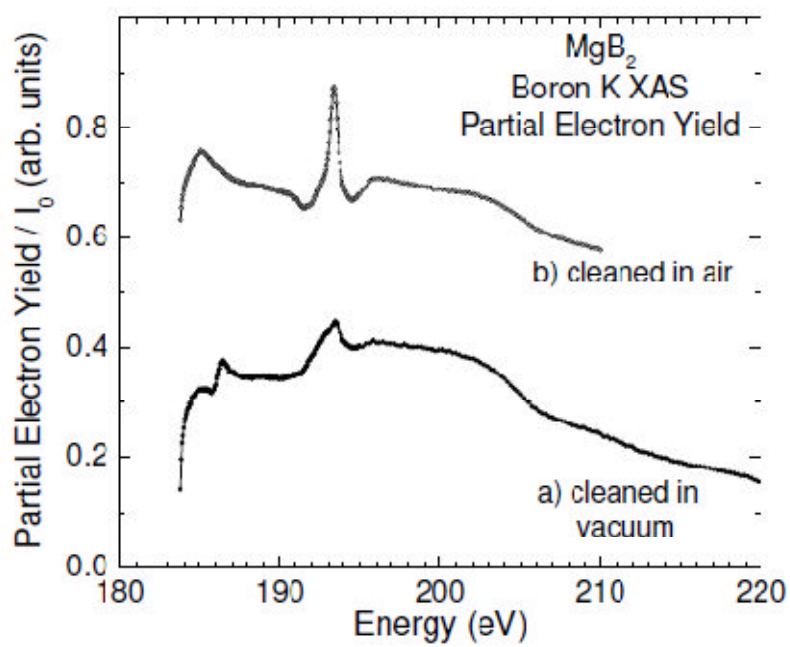


Fig. 4

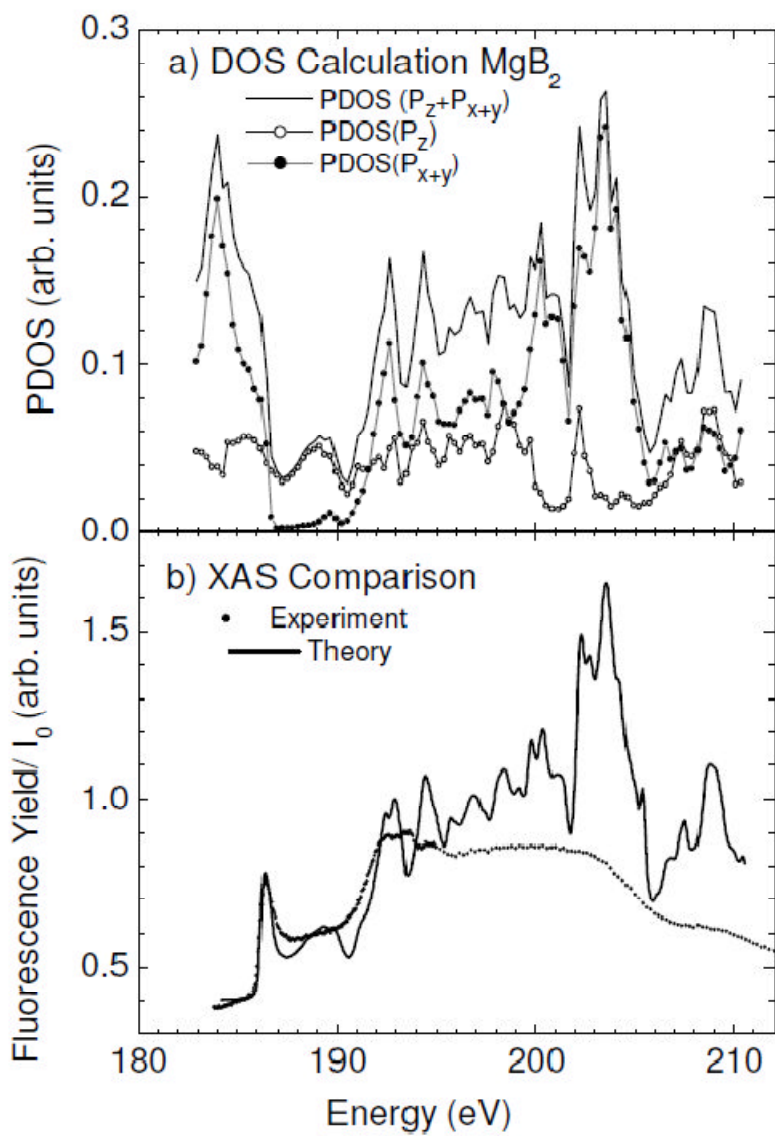


Fig. 5